

Interactions between NF κ B and Its Inhibitor κ B: Biophysical Characterization of a NF κ B/ κ B- α Complex

Tiansheng Li,¹ Linda O. Narhi,^{1,3} Jie Wen,¹ John S. Philo,^{1,*} Karen Sitney,¹
Jun-ichiro Inoue,² Tadashi Yamamoto,² and Tsutomu Arakawa^{1,*}

Received May 1, 1998

The N-terminal domain (1–318 amino acids) of mouse NF κ B (p65) has been purified to homogeneity from the soluble fraction of *Escherichia coli* cells expressing this protein. Its complex with a full-length κ B- α (MAD3, 1–317 amino acids) molecule was generated by binding the *E. coli*-derived κ B- α to the purified NF κ B and purifying the complex by sequential chromatography. The stoichiometry of NF κ B to κ B in the complex was determined to be 2 to 1 by light scattering and SDS–polyacrylamide gel electrophoresis. The secondary structure of the NF κ B (p65) determined by Fourier-transform infrared (FTIR) spectroscopy is in good agreement with that of the p50 in the crystal structure of the p50/DNA complex, indicating that no significant structural change in NF κ B occurs upon binding of DNA. The FTIR spectrum of the NF κ B/ κ B complex indicates that its secondary structure is composed of 17% α -helix, 39% β -strand, 18% irregular structures, and 26% β -turns and loops. By comparing these data to the FTIR data for NF κ B alone, it is concluded that the κ B (MAD3) in the complex contains 35% α -helix, 27% β -strand, 22% irregular structures, and 16% β -turns and loops. Circular dichroism (CD) analysis of a shorter form of κ B (pp40) indicates that it contains at least 20% α -helix and that the κ B subunit accounts for nearly all of the α -helix present in the NF κ B/ κ B complex, consistent with the FTIR results. The stabilities of NF κ B, κ B, and their complex against heat-induced denaturation were investigated by following changes in CD signal. The results indicate that the thermal stability of κ B is enhanced upon the formation of the NF κ B/ κ B complex.

KEY WORDS: NF κ B; κ B; FTIR; CD; light scattering; solution structure; thermal stability.

1. INTRODUCTION

NF κ B was first identified as a DNA-binding protein specific for the 10-base-pair κ B site in the immunoglobulin κ -light-chain enhancer of B lymphocytes (Sen and Baltimore, 1986). It is a heterodimeric complex composed of two subunits, the p65 protein and the p50 protein, and

exists in an inactive cytoplasmic form, bound to its inhibitor κ B (Baldwin, 1996). The members of the NF κ B transcription factor family share a high sequence homology in the N-terminus (approximately 300 amino acids) termed the “rel homology region,” involved in DNA binding, dimerization, and nuclear localization. Upon induction by cellular stress factors such as tumor necrosis factor and agents such as lipopolysaccharide and hydrogen peroxide, phosphorylation of κ B occurs and this inhibitor is subsequently targeted for degradation and dissociation from the NF κ B/ κ B complex (Brockman *et al.*, 1995; Brown *et al.*, 1995; Chen *et al.*,

¹ Departments of Small Molecule Chemistry and Process Science, Amgen Inc., Thousand Oaks, California 91320.

² University of Tokyo, Institute of Medical Science, 4-6-1, Shirokanedai, Tokyo 108, Japan.

³ To whom correspondence should be addressed; e-mail: Lnarhi@amgen.com.

* Current address: Alliance Protein Laboratories, 3957 Corte Cancion, Thousand Oaks, Ca. 91360.

⁴ Abbreviations: FTIR, Fourier transform infrared; CD, circular dichroism; GST, glutathione S-transferase; SDS–PAGE, sodium dodecylsulfate–polyacrylamide gel electrophoresis.

1995; Traenckner *et al.*, 1995). An κB - α -specific kinase has recently been identified (Chen *et al.*, 1996; DiDonato *et al.*, 1997). Upon dissociation of κB , the p65/p50 heterodimer is translocated into the nucleus, where it activates gene expression.

Recently, the crystal structure of an NF κB /DNA complex composed of the p50 homodimer and a κB site has been determined (Ghosh *et al.*, 1995; Muller *et al.*, 1995). The crystal structure of the p50/DNA complex revealed that the protein-DNA interface involves five loop regions consisting mostly of positively charged protein side chains from the p50 protein. Based on the crystal structure of the p50/DNA complex and the published mutagenesis data of κB , it was proposed that the κB molecule may bind to NF κB domains near the DNA-binding loop regions so as to inhibit DNA binding. The NF κB domains interacting with κB may also contain the signal regions responsible for nuclear translocation. The mutational studies of κB (pp40) demonstrated that ankyrin repeats alone are not sufficient to inhibit the DNA-binding activity of NF κB , and that the C-terminal region of pp40 is required to manifest κB biological activity (Inoue *et al.*, 1992). However, direct structural information on isolated κB and the NF κB / κB complex is thus far very limited. To further investigate the interactions between NF κB and its inhibitor κB , we purified the complex of the N-terminal region (318 amino acids) of the mouse p65 protein with a full-length human κB - α (MAD3) molecule as well as the p65 protein alone. We also purified a short form of the chicken κB (pp40) molecule that shares extensive sequence homology with MAD3, but contains only five ankyrin repeats. Biophysical characterizations, including Fourier-transform infrared (FTIR),⁴ CD spectroscopy, and light scattering analysis, of the NF κB / κB complex and its protein subunits were carried out to probe the structural aspects of the NF κB and κB molecules in the protein complex.

2. EXPERIMENTAL PROCEDURES

2.1. Protein Purification

The N-terminal region (318 amino acids) of the mouse p65 protein was expressed in *Escherichia coli* as a fusion protein with glutathione-S-transferase (GST) at the N-terminus. Three chromatographic steps, glutathione-sepharose, S-sepharose, and gel filtration, were used following thrombin cleavage to purify the NF κB protein from the soluble fraction. The NF κB complex was purified using two columns, glutathione-sepharose and S-

sepharose, after thrombin cleavage. The complex was further purified by gel filtration on a Superdex 200 column (Pharmacia). The truncated pp40 protein was expressed as a GST fusion to amino acids 69–254 of pp40 in which the tryptophan residue at position 70 and the tyrosine residue at position 254 were both mutated to serines (GST-ANK- κB ; Inoue *et al.*, 1992). It was purified following a procedure similar to that described for the NF κB fusion protein.

2.2. FTIR Spectroscopy

NF κB (p65) in 10 mM Tris-HCl, 100 mM NaCl, pH 7.3, was concentrated and hydrogen-deuterium exchanged into 10 mM sodium phosphate, 150 mM NaCl, pD 7.0 buffer using Centricons (Amicon). Typically, 1024 interferograms were coadded and Fourier-transformed at a spectral resolution of 4 cm^{-1} by employing a Mattson Research Series Model 1000 spectrometer with an MCT detector cooled by liquid nitrogen. The spectrometer was continuously purged with dry air to eliminate the spectral contribution of atmospheric water vapor. Sample temperatures of up to 90°C were controlled by a thermal controller (Boulder Nonlinear System, Inc.). IR spectral analyses including self-Fourier deconvolution and curve-fitting were carried out by employing Grams/386 and Spectral Calc software (Galatic Industries Co.).

2.3. CD Spectroscopy

The CD spectra were determined on a Jasco J-720 spectropolarimeter controlled by a DOS-based computer and Jasco software using cylindrical cuvettes with a pathlength of 0.02 cm for the far-UV region (250–190 nm). Thermal denaturation was performed on the same instrument using a Peltier thermal control JTC-343 unit, a heating rate of 20°C/hr, and rectangular cuvettes with a pathlength of 0.1 cm. Changes in structure with incubation at a single temperature were determined on the same instrument with the rectangular cuvettes, with the Peltier unit set at 27, 38, and 45°C, collecting ellipticity at a single wavelength. Protein samples of 0.2 mg/ml for pp40, 0.6 mg/ml for the NF κB / κB complex, and 0.4 mg/ml for NF κB alone were used, so that the concentration of the proteins analyzed individually corresponded to the concentration of the proteins in the complex.

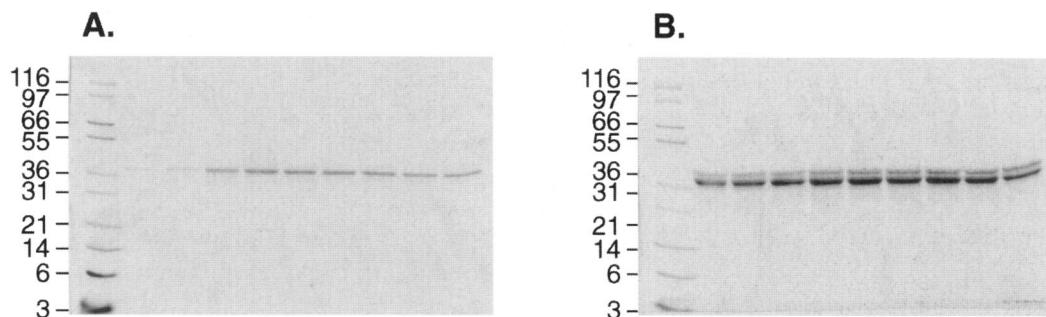


Fig. 1. SDS-PAGE of NF κ B (p65) (A) and NF κ B/MAD3 complex (B) under reducing conditions. (A) NF κ B fractions from Superose-12 column; (B) fractions of NF κ B/MAD3 complex from Superdex 200 column.

2.4. Light Scattering

The instrumentation and methods of data analysis and calibration were described previously (Arakawa *et al.*, 1994; Philo *et al.*, 1994). Briefly, we used three detectors in series following a size exclusion chromatography column; i.e., light scattering, absorbance at 280 nm, and refractive index. By using the signals from all three detectors, together with the protein extinction coefficients, we are able to determine the molecular weight of the complex. For these studies, a Superdex 200 column (Pharmacia) was used with phosphate-buffered saline, pH 6.5, as the eluent, at a flow rate of 0.5 ml/min.

3. RESULTS AND DISCUSSION

3.1. Stoichiometric Ratios of NF κ B and κ B in the Complex

The purified NF κ B was subjected to Superose-12 (Pharmacia) column chromatography and the eluates were analyzed by SDS-PAGE as shown in Fig. 1A. They contain essentially a single band at 38,000 Da. The purified NF κ B/MAD3 complex eluted from the Superdex 200 column as a single peak which contained two distinct bands upon reducing SDS-PAGE analysis. The lower band has twice the intensity of the upper one (Fig. 1B). The upper band was identified as MAD3 and the lower one as NF κ B by comparison with the migration of NF κ B alone (Fig. 1A). Protein sequencing and Western blot analysis using anti-NF κ B and anti- κ B polyclonal antibodies also confirmed that the lower band on SDS-PAGE is NF κ B, while the upper one is MAD3 (data not shown). The peak fraction eluting from the Superdex 200 column was subjected to light scattering analysis (Fig. 2). Since both proteins in the complex are

unglycosylated, the molecular weight can be calculated from the combined light scattering data and refractive index signal, and was determined to be 113,000 Da for the NF κ B/MAD3 complex. The calculated molecular weights for both NF κ B and κ B are about 36,000 Da, and thus the complex appears to be composed of three subunits. The SDS-PAGE analysis indicates that two subunits are NF κ B and one is MAD3. Data analysis using all three signals combined excludes the 1 NF κ B:2 MAD3 stoichiometry. This conclusion is consistent with the existing model that one κ B is bound to an NF κ B dimer.

3.2. Structural Characterizations of NF κ B and the NF κ B/ κ B Complex

3.2.1. The Secondary Structures of NF κ B (p65) Protein

Figure 3 shows the Fourier self-deconvolved IR spectrum and the curve-fitted components in the amide I' region of NF κ B. The peak position of the amide I' band is at 1637 cm^{-1} , indicating that NF κ B contains mostly β -strands. The curve-fitted results (see also Table I) of the amide I' bands indicate that the NF κ B contains approximately 45% β -strands, 16% irregular structures, 21% loops, 10% β -turns, and only 8% α -helix. This assignment of the secondary structure of the NF κ B (p65) protein is in reasonable agreement with the crystal structure of the p50 protein in the NF κ B/DNA complex (Ghosh *et al.*, 1995), which indicated that the p50 protein contained about 38% β -strands, 7% α -helix, and 55% irregular structures, loops, and β -turns. Since p65 and p50 share extensive homology, it is unlikely that the p65 protein undergoes significant structural changes upon binding to the κ B site.

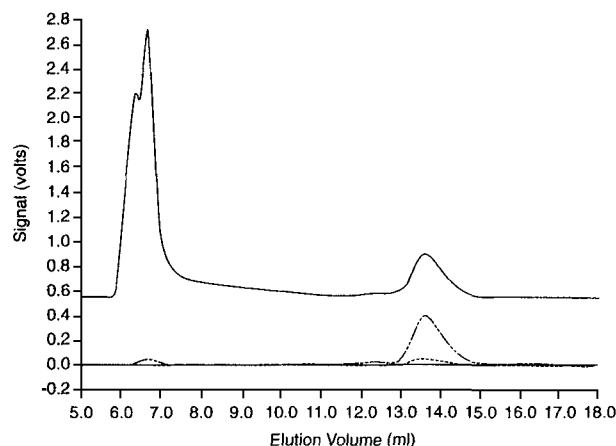


Fig. 2. Light scattering profile of NF κ B/MAD3 complex. Solid line: total light scattering at 90° angle; long-dashed line: measured refractive index at 633 nm; short-dashed line: measured absorbance at 280 nm.

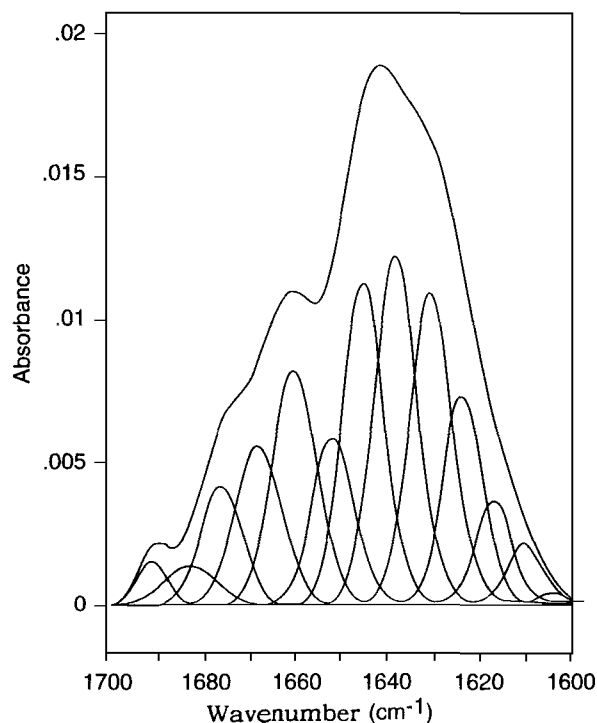


Fig. 3. FTIR spectrum in the amide I' region (1600–1700 cm^{-1}) of NF κ B, showing the curve-fitted spectrum and the individual components.

3.2.2. Secondary Structures of NF κ B/MAD3 Complex

Figure 4 shows the Fourier self-deconvolved IR spectrum and the curve-fitted components in the amide I' region of the NF κ B/MAD3 complex. The peak position of amide I' of the complex is near 1645 cm^{-1} , which

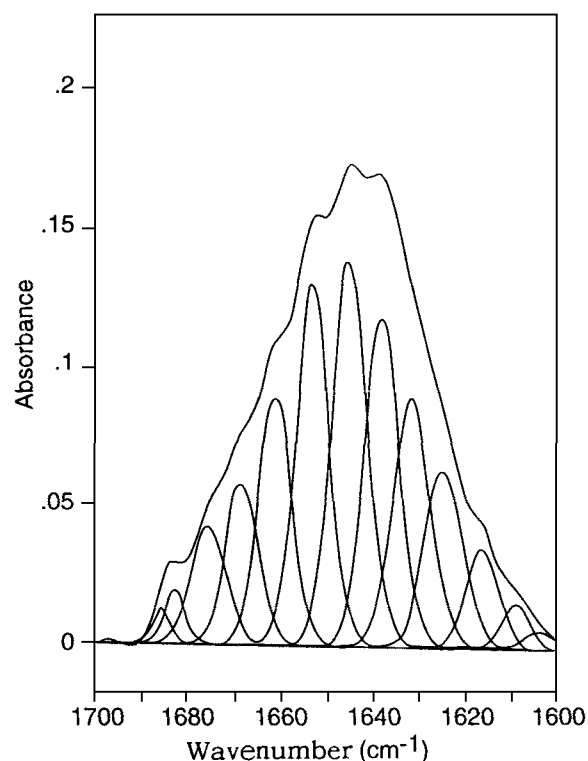


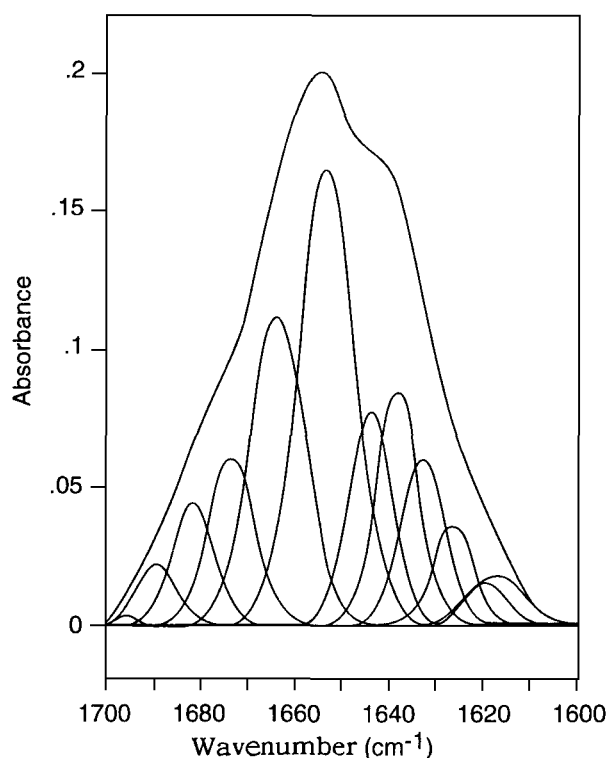
Fig. 4. FTIR spectrum in the amide I' region (1600–1700 cm^{-1}) of NF κ B/MAD3, showing the curve-fitted spectrum and the individual components.

is 8 cm^{-1} higher than that of NF κ B alone. As shown in Table I, the secondary structures present in the NF κ B/MAD3 complex consist of 39% β -strands, 18% irregular structures, 18% loops, 8% β -turns, and 17% α -helix. There appear to be no significant changes in the secondary structure of NF κ B upon binding to the κ B site; there would also be no significant changes in the secondary structure of NF κ B upon MAD3 binding, based on the assumption that the secondary structures of MAD3 in the complex were determined to be composed of about 35% α -helix, 27% β -strands, 22% irregular structures, 12% loops, and 4% β -turns.

To compare the structural similarity of the full-length MAD3 protein with an κ B (pp40) protein that contains only the five ankyrin repeats, the secondary structure of the isolated truncated pp40 protein was also determined by FTIR spectroscopy. Figure 5 shows the Fourier self-deconvolved IR spectrum and the curve-fitted components in the amide I' region of the pp40 protein. The curve-fitting results, listed in Table I, show that the isolated pp40 protein contains approximately 27% β -strands, 10% irregular structures, 18% loops, 17% β -turns, and 28% α -helix.

Table I. Estimated Protein Secondary Structures of NFκB, pp40, and NFκB/MAD3 Complex from Curve-Fitting Data of Amide I' Bands

(NFκB) ₂ /MAD3 complex			NFκB			pp40		
ν (cm ⁻¹)	A (%)	Type	ν (cm ⁻¹)	A (%)	Type	ν (cm ⁻¹)	A (%)	Type
1616	4	β-Strand	1617	4	β-Strand	1617	3	β-Strand
1625	9	β-Strand	1623	9	β-Strand	1620	2	β-Strand
1631	13	β-Strand	1630	15	β-Strand	1627	4	β-Strand
1638	13	β-Strand	1638	17	β-Strand	1633	7	β-Strand
1645	18	Irregular	1645	16	Irregular	1638	11	β-Strand
1653	17	α-Helix	1652	8	α-Helix	1644	10	Irregular
1661	11	Loops	1660	12	Loops	1653	28	α-Helix
1668	7	Loops	1668	9	Loops	1664	18	Loops
1676	5	β-Turns	1676	6	β-Turns	1674	8	β-Turns
1683	2	β-Turns	1683	3	β-Turns	1682	6	β-Turns
1687	1	β-Turns	1691	1	β-Turns	1689	3	β-Turns

**Fig. 5.** FTIR spectrum in the amide I' region (1600–1700 cm⁻¹) of pp40, showing the curve-fitted spectrum and the individual components.

Similar results were obtained when the secondary structure was analyzed by CD spectroscopy, with the pp40 ικB containing at least 20% α-helix, and accounting for nearly all of the α-helix in the complex (data not shown). Since the isolated MAD3 protein is not available at this point, it is not clear if the increased percentage of α-helix in the bound MAD3, by comparison

to that of pp40, is due to the portion of the MAD3 structure not present in the pp40 protein or to the conversion of the irregular structures to α-helix in MAD3 upon binding by NFκB, or alternatively to changes in NFκB secondary structure induced by complex formation.

Interestingly, we have observed that in the absence of reducing agent MAD3 forms a covalent disulfide bond with one subunit of the p65 protein in the complex as observed by nonreducing SDS-PAGE analysis (data not shown). Examination of the MAD3 sequence shows that one Cys located in the N-terminal domain may be a potential candidate for the disulfide link to p65, since this region contains a cluster of negatively charged amino acids and hence is expected to be highly solvent-exposed.

3.3. Thermal Stability of NFκB/ικB Complex

To assess the effect of complex formation on the structural integrity of ικB and NFκB, we examined the thermal stability of α-helix in the isolated pp40 and NFκB/MAD3 complex by CD spectroscopy. Figure 6 shows the temperature dependence of CD ellipticity measured at 222 nm for the NFκB and at 230 nm for the ικB and the NFκB/ικB complex. The isolated pp40 protein appears to be denatured at lower temperatures than NFκB and the NFκB/MAD3 complex, as demonstrated by the midpoint of the melting curves. The determined T_m is approximately 45°C for pp40, 52°C for the NFκB, and 51°C for NFκB/MAD3 complex. It is therefore concluded that the formation of complex does stabilize the α-helical conformation in ικB, but has little effect on the stability of NFκB, suggesting that complex dissociation occurs around the melting temperature of the NFκB.

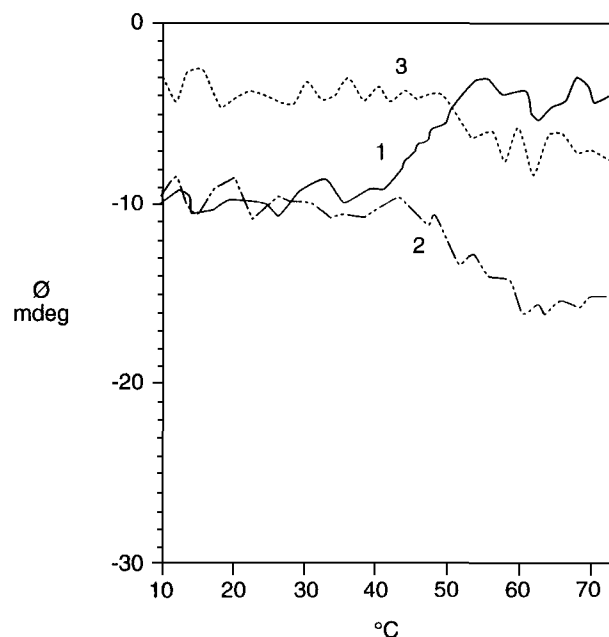


Fig. 6. Thermal stability of secondary structure as monitored by CD. Ellipticities measured at 222 nm for pp40 (—, 1), 215 nm for NFκB (- - -, 2) and the NFκB/MAD3 complex (- · -, 3) as the temperature increased from 10 to 70°C.

The stability of the proteins to incubation at 37°C (below the T_m for all three proteins) was also compared (Fig. 7). The MAD3 undergoes a gradual loss of ellipticity during the first 30 min of incubation at 37°C, after which the signal remains constant, while the NFκB undergoes an even more gradual loss of CD signal over the first 60 min. In contrast, the complex containing concentrations of ικB and NFκB similar to the individual proteins analyzed above maintains a constant signal over 3 hr at 37°C. This suggests that the free ικB is unstable at physiological temperature, and is stabilized by complex formation. When the three protein samples were incubated at 27 and 45°C, similar results were obtained.

4. CONCLUSIONS

In conclusion, we have purified an NFκB/ικB complex to homogeneity and determined that the NFκB and ικB-α (MAD3) form a 2:1 complex, which confirms the existing molecular model proposed in the literature. Secondary structures of the NFκB/ικB complex were determined by FTIR and CD spectroscopy. The NFκB molecule studied here (N-terminal 318 amino acids of p65) has a secondary structure similar to the crystallized

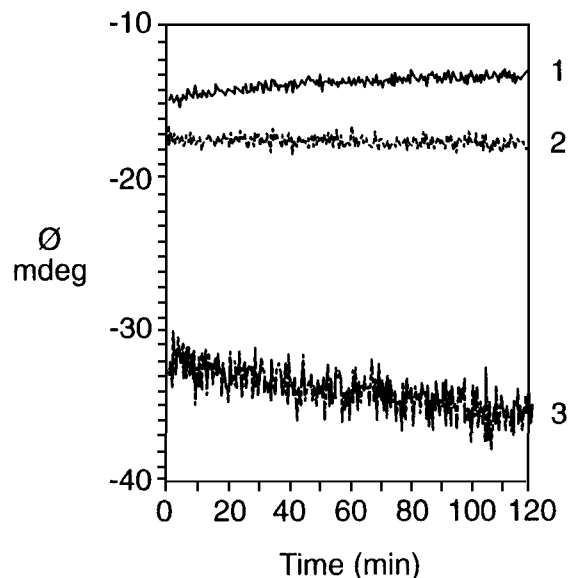


Fig. 7. Stability of NFκB, ικB, and their complex at physiological temperature. Ellipticities were monitored at 37°C with time, at 222 nm for pp40 (—, 1), 215 nm for NFκB/MAD3 (- - -, 2) and 222 nm for NFκB (- · -, 3).

p50, consisting of mostly β-strands and little α-helix. We determined that α-helix is the dominant secondary structure (35%) in the ικB proteins MAD3 and pp40. Free ικB is thermally unstable (loss of α-helix) at physiological temperature, but the α-helical conformation of ικB is stabilized to temperature-induced denaturation within the NFκB/ικB complex. Thus, it is possible that the minor conformational changes in ικB induced by complex formation with NFκB protect it from degradation, and that dissociation results in a conformation which is susceptible to rapid degradation, and therefore turnover within the cell.

ACKNOWLEDGMENTS

The authors wish to thank Danette Baron for preparation of the figures, and Joan Bennett for preparation of the manuscript.

REFERENCES

- Arakawa, T., Wen, J., and Philo, J. S. (1994). *Arch. Biochem. Biophys.* **308**, 267–273.
- Baldwin, A. S. (1996). *Annu. Rev. Immunol.* **14**, 649–681.

- Brockman, J. A., Scherer, D. C., Hall, S. M., McKinsey, T. A., Qi, X., Lee, W. Y., and Ballard, D. W. (1995). *Mol. Cell. Biol.* **15**, 2809–2818.
- Brown, K., Gerstberger, S., Carlson, L., Franzoso, G., and Siebenlist, U. (1995). *Science* **267**, 1485–1491.
- Chen, Z. J., Hagler, J., Palombella, V., Melandri, F., Scherer, D., Ballard, D., and Maniatis, T. (1995). *Genes Dev.* **9**, 1586–1597.
- Chen, Z. J., Parent, L., and Maniatis, T. (1996). *Cell* **84**, 853–862.
- DiDonato, J. A., Hayakawa, M., Rothwarf, D. M., Zandi, E., and Harin, M. (1997). *Nature* **388**, 548–554.
- Ghosh, G., Van Duyne, G., Ghosh, S., and Sigler, P. B. (1995). *Nature* **373**, 303–310.
- Inoue, J.-I., Kerr, L. D., Rashid, D., Davis, N., Bose, H. R., Jr., and Verma, I. M. (1992). *Proc. Natl. Acad. Sci. USA* **89**, 4333–4337.
- Muller, C. W., Rey, F. A., Sodeoka, M., Verdine, G. L., and Harrison, S. C. (1995). *Nature* **373**, 311–317.
- Philo, J. S., Talvenheimo, J., Wen, J., Rosenfeld, R., Welcher, A., and Arakawa, T. (1994). *J. Biol. Chem.* **269**, 27840–27846.
- Sen, R., and Baltimore, D. (1986). *Cell* **46**, 705–716.
- Traenckner, E. B.-M., Pahl, H. L., Henkel, T., Schmidt, K. N., Wilk, S., and Baeuerle, P. A. (1995). *EMBO J.* **14**, 2876–2883.